Ground-state properties of antiferromagnetic anisotropic $S = 1$ Heisenberg spin chains

D. Peters

Institut für Theoretische Physik, RWTH Aachen University, 52056 Aachen, Germany

I. P. McCulloch

Centre for Engineered Quantum Systems, School of Mathematics and Physics, The University of Queensland, St. Lucia, QLD 4072, Australia

W. Selke

Institut für Theoretische Physik, RWTH Aachen University and JARA-HPC, 52056 Aachen, Germany

Using (infinite) density-matrix renormalization-group techniques, ground-state properties of antiferromagnetic $S = 1$ Heisenberg spin chains with exchange and single-site anisotropies in an external field are studied. The phase diagram is known to display a plenitude of interesting phases. We elucidate quantum phase transitions between the supersolid and spin-liquid phases as well as the spin-liquid and ferromagnetic phases. Analyzing spin-correlation functions in the spin-liquid phase, commensurate and (two distinct) incommensurate regions are identified.

I. INTRODUCTION

In recent years, ground-state properties of the antiferromagnetic Heisenberg spin-1 chain with single-site and uniaxial exchange anisotropies in an external field have been investigated rather extensively.[1–5] The model is described by the Hamiltonian

$$\mathcal{H} = \sum_i \left[J \left(S_i^x S_{i+1}^x + S_i^y S_{i+1}^y + \Delta S_i^z S_{i+1}^z \right) + D \left(S_i^z \right)^2 - B S_i^z \right], \quad (1)$$

where i denotes the lattice sites, Δ denotes the exchange, and D denotes the single-site anisotropy. The external field B acts along the z direction.

The magnet displays various intriguing phases at zero temperature (and, thence, corresponding quantum phase transitions): the antiferromagnetic (AF), ferromagnetic (F), half-magnetization plateau (HMP), spin-liquid (SL), supersolid (SS), and "large-D" phases. Some of these phases, the AF, F, SL, and SS phases, show up in the corresponding classical Heisenberg model,[3,4,6] while the HMP and large-D phases reflect the discretization of the spin orientations in the quantum case. The theoretical efforts have been motivated and inspired, partly, by related experiments.[7,8]

Perhaps most attention, in the context of this, Eq. (1), and similar[9–14] models, has been paid to the supersolid phase,[15] being the analog of the "mixed" or "biconical"[16] phase in the classical limit.[17,18] Note that a mapping from quantum lattice gases to magnetic systems, explaining the term "supersolid" for magnets, has been introduced some decades ago.[19] Typically, quantum fluctuations tend to reduce substantially the range of stability of the supersolid phase,[4,9] as compared to the classical variant.

The spin correlations in the supersolid phase of the anisotropic Heisenberg spin chain, Eq. (1), have been argued to behave like in a Luttinger liquid, with algebraic spatial decay.[2] Magnetization profiles have revealed the close analogy of the supersolid to the corresponding classical biconical structures.[3,4] The critical exponent of the spin stiffness,

describing the transition to the bordering AF and HMP phases, has been found[2,5] to be 1/2.

In this contribution, we shall consider interesting aspects of the model (1) which have not been studied in detail so far. We shall deal with the transition between the supersolid and the spin-liquid phases as well as with the SL-F quantum phase transition. Both transitions have not been analyzed before for this model. In addition, spin correlations in the SL phase will be analyzed, to clarify, especially, previous suggestions on distinguishing commensurate (C) and incommensurate (IC) regions in that phase.[1,3,4]

In the present study, mainly infinite density-matrix renormalization-group (iDMRG) techniques[20–22] have been used, with systematic enlargening on the number of matrices in the matrix product states. In general, the chosen size of the matrices is an important parameter determining the reliability of the calculation. Here, the dimension M of the largest matrices ranges, typically, from 50 to 500. The truncation error varies in between 10^{-6} and 10^{-10}. In a few cases, results are compared to ones we obtain from DMRG calculations for finite chains, with open boundary conditions, of length L, with $L \leqslant 128$.

II. TRANSITION BETWEEN SUPERSOLID AND SPIN-LIQUID PHASES

Following previous analyses[1–5] of the model (1), we focus on two cases: at a fixed ratio between the two types of anisotropies, $D/J = \Delta/2$, and at a given, quite large exchange anisotropy, $\Delta = 5$, with varying single-site anisotropy D/J. The corresponding ground-state phase diagrams (or parts thereof) have been obtained before,[1–5] using DMRG and quantum Monte Carlo techniques. In both cases, the phase diagrams include the AF, F, HMP, SL, and SS phases. The supersolid phase results from competing uniaxial, along the z axis, exchange, $\Delta > 1$, and planar single-site, $D > 0$, anisotropies.

The supersolid phase may be bordered by massive, AF or HMP, or by critical, SL, phases.[2–5] The transitions to the massive phases have been investigated in detail before.[2,5]
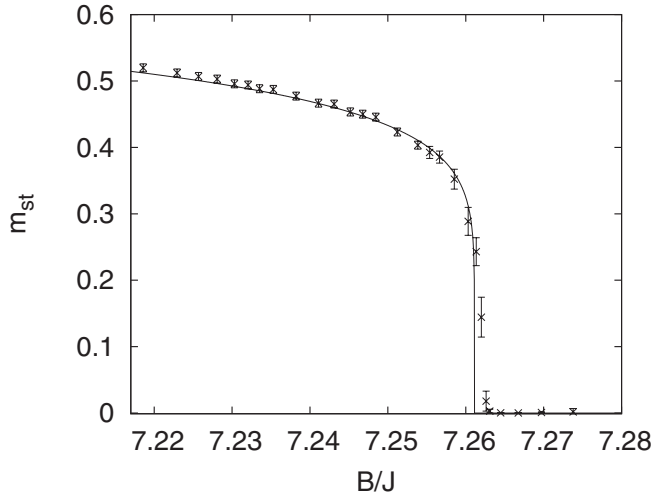
FIG. 1. Staggered magnetization m_{st} vs external field B/J at $D/J = \Delta/2 = 2.5$ near the supersolid to spin-liquid transition. For comparison, a power-law fit to the iDMRG data with the critical exponent $\beta = 1/8$ is shown (see text).

Here we discuss the transition from the supersolid to the spin-liquid phase, the SS-SL transition. As illustrated in Fig. 1 for $\Delta = 2D/J = 5$, the transition seems to belong to the two-dimensional classical Ising universality class. The critical exponent β, describing the vanishing of the staggered magnetization m_{st} at the transition, is, indeed, consistent with the famous Onsager value $\beta = 1/8$. Actually, we did a χ^2 fit of our iDMRG data in the range $7.22 < B/J < 7.262$ to the form $m_{st} = a(B_c/J - B/J)^{1/8}$. We obtain $B_c \approx 7.262$, as shown in Fig. 1. The critical field has been also determined by analyzing the entanglement entropy, leading to a consistent estimate. Note the (small) deviation extremely close to B_c, which one may attribute to discretization error in determining the magnetic field or to insufficient size of the matrix dimension M, $M \leqslant 500$, in this regime near the transition.

In addition, we also identify an Ising-like sector near the SS-SL transition, with exponentially decaying longitudinal spin correlations up to rather large distances, as will be discussed below. Note that our suggestion on the universality class of the SS-SL transition is in line with a corresponding finding on a related two-dimensional quantum anisotropic Heisenberg antiferromagnet, where the supersolid to spin-liquid transition has been concluded to be in the universality class of the three-dimensional Ising case.[11] It is worth mentioning that both suggestions, for quantum magnets in dimensions $d = 1$ and 2 at zero temperature, agree with the well-known dimensional argument[23] relating critical exponents in d-dimensional quantum systems to those in corresponding $(d + 1)$-dimensional classical systems. Indeed, here the classical transitions between the biconical and spin-flop phases are of the Ising type.[6,16]

III. CORRELATION FUNCTIONS IN THE SPIN-LIQUID PHASE

Before turning to the discussion of the SL-F quantum phase transition, let us first consider characteristics of the SL phase. As has been noted before,[1,3,4] the Hamiltonian (1) may

describe both commensurate (C) and incommensurate (IC) spin-liquid structures, as has been inferred from the behavior of energy gaps[1] and magnetization profiles.[3,4]

In this study, we shall present direct evidence for both types of structures in the spin-liquid phase by analyzing, especially, longitudinal $\Gamma_z(r) = \langle S_i^z S_{i+r}^z \rangle$ spin-correlation functions. Asymptotically, $r \longrightarrow \infty$, Γ_z acquires the value m^2, where m is the total magnetization per site. For sufficiently large distances r, the dominant algebraically decaying terms of the correlations are expected[24] to be either of, due to magnetization fluctuations, commensurate form, $\propto 1/r^2$, or of incommensurate form, $\propto (1/r^\eta) \cos(qr)$, with $\eta < 2$, as usual for Luttinger liquids. Such a behavior is confirmed by our iDMRG calculations. In the IC case, we find the wave number q to be related to the total magnetization per site, m, in two distinct ways: We obtain either $q_1 = \pi(1 - m)$ [(IC)$_1$] or $q_2 = 2\pi(1 - m)$ [(IC)$_2$], setting the lattice constant equal to one.

Examples of longitudinal correlation functions of type C, (IC)$_1$, and (IC)$_2$ are depicted in Fig. 2, for selected values of D/J and m, fixing the exchange anisotropy, $\Delta = 5$. Note that, in the example for the C case, Γ_z shows roughly an exponential decay with oscillations at small distances r, approaching the monotonic algebraic decay, $\propto 1/r^2$, only at larger separations.

Varying systematically the single-site anisotropy D and the magnetization m, at $\Delta = 5$ (compare to Ref. 1), one may then identify three different regions, C, (IC)$_1$, and (IC)$_2$, in the $(D/J,m)$ plane, as shown in Fig. 3. Note that the IC structures tend to occur close to the F phase. Obviously, there the longitudinal spin correlations are expected to decay rather slowly. Accordingly, the exponent η is small, and the oscillatory part of the long-range correlations may dominate the monotonic part being proportional to $1/r^2$. At sufficiently small negative values of D, one observes the (IC)$_1$ region. This region may be subdivided into two parts: At larger magnetizations, we observe ferroquadrupolar ordering,[25–27] where the algebraic decay of the four-point transverse cor-
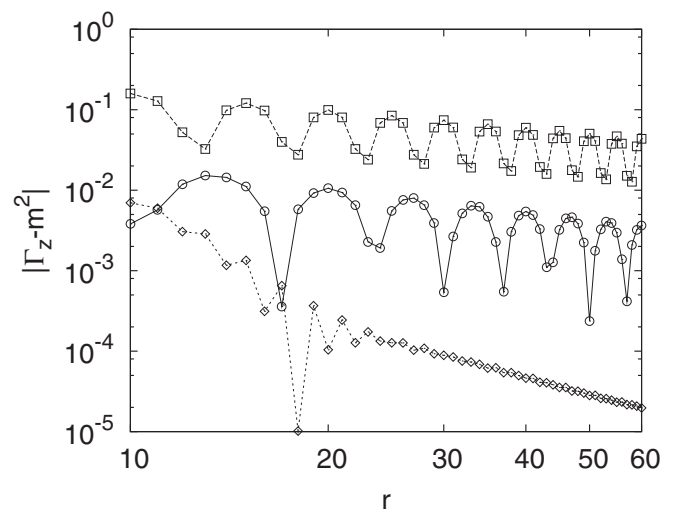

FIG. 2. Longitudinal spin-correlation function $|\Gamma_z - m^2|$ vs separation distance r, at $\Delta = 5$, with (a) $D/J = 2.5$, $m = 23/40$ (circles), (IC)$_1$ type, (b) $D/J = -1.5$, $m = 1/5$ (squares), (IC)$_1$ type, and (c) $D/J = 1$, $m = 4/10$ (diamonds), C type. Interpolating lines are guides to the eye.
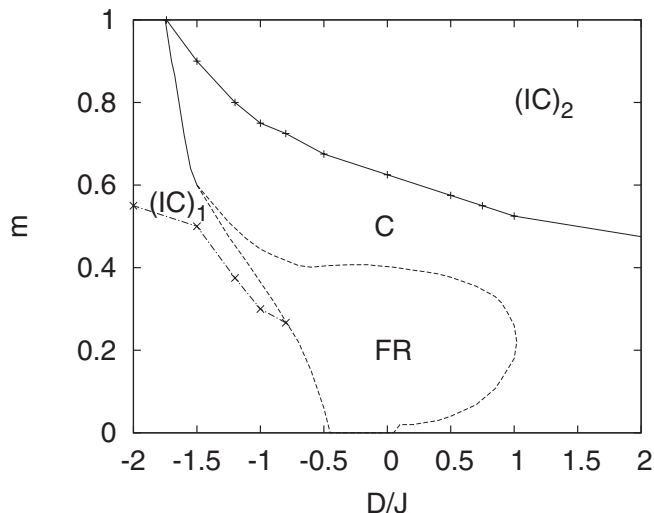
FIG. 3. Solid boundary lines separating C and IC regions in the $(D/J,m)$ plane at $\Delta = 5$. The dashed line sketches, as a guide to the eye, the border of the forbidden region (FR) (see Ref. [1]). The dashed-dotted line in the $(IC)_1$ phase divides ferroquadrupolar ordering, at high m, from spin-density-wave ordering.

relation function $\langle (S_i^+)^2 (S_{i+r}^-)^2 \rangle$ is slower than that of $\Gamma_z(r)$, due to a smaller exponent η. At lower magnetizations, one encounters a spin-density-wave ordering, with the longitudinal spin correlations being dominant. This behavior is exemplified in Fig. 4. The $(IC)_2$ region occurs at larger values of D/J. In between the two IC regions, the commensurate region intervenes. There, the exponent η characterizing the algebraic decay of Γ_z with spatially modulated behavior is larger than two. Asymptotically, for large distances r, the dominant algebraic term is then proportional to $1/r^2$, decaying monotonically. Indeed, the changeover between the C and IC regions may be conveniently monitored by determining the exponent η from fits of the iDMRG data for the longitudinal spin correlations.[27]
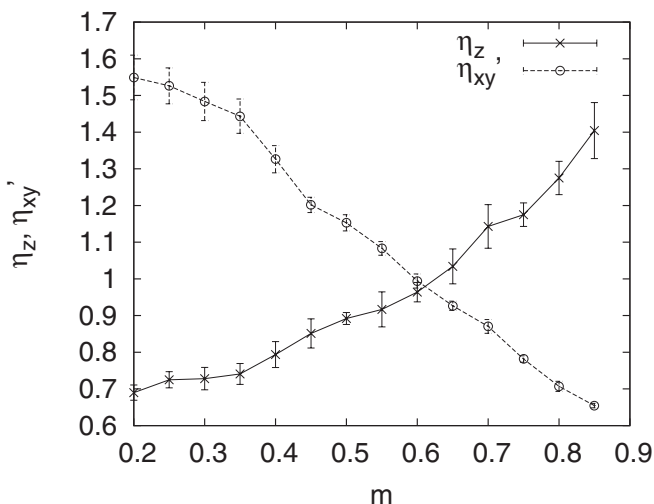

FIG. 5. Exponent η_z for the oscillatory part of the algebraically decaying longitudinal spin correlations Γ_z vs magnetization m at $\Delta = 5$ and various values of D/J.

A few examples, at several fixed values of D/J and changing m, are displayed in Fig. 5 (compare to Fig. 3).

The "forbidden region" (FR) in the $(D/J,m)$ plane, which has been sketched in Fig. 3, gives rise to first-order transitions.

Our calculations on the spin correlations in the $(D/J,m)$ plane confirm and refine substantially previous findings,[1] where the $(IC)_2$ region seems to have been overlooked. Similarly, there has been no mentioning of the two distinct parts of the $(IC)_1$ phase and of the supersolid phase which shows up at fairly low magnetizations and sufficiently large values of D/J, as we have discussed before.[4] We omitted the supersolid phase in Fig. 3, for reasons of simplicity.

Close to the supersolid to spin-liquid transition, the longitudinal spin correlations are governed, up to quite large distances, by an exponential decay with π oscillations, signaling, presumably, the above-mentioned Ising sector. Further details are presented elsewhere.[27]

FIG. 4. Comparing the exponents for the decay of two-spin longitudinal, η_z, and four-spin transverse, η'_{xy}, correlations to identify the extent of the regions with ferroquadrupolar and spin-density-wave orderings, at $D/J = -2$ and $\Delta = 5$.
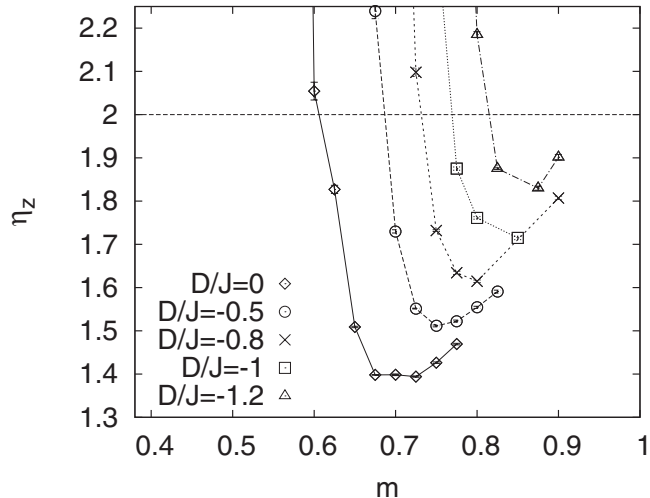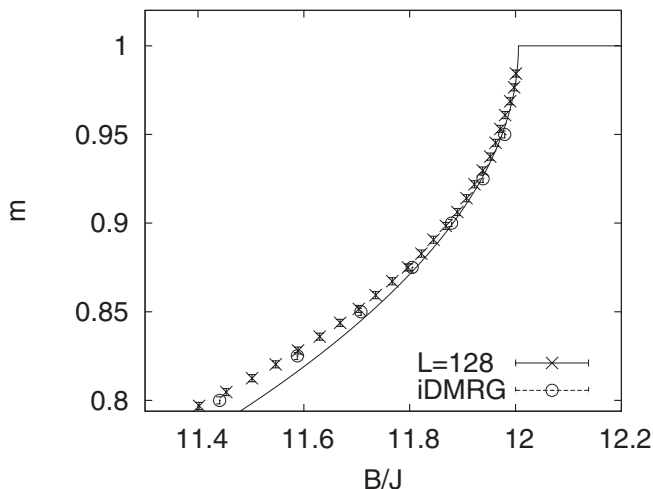

FIG. 6. Magnetization m vs field B close to the SL-F transition at $\Delta = 5$ and $D = 0$. Data from iDMRG and finite-size DMRG, for $L = 128$ sites, calculations are shown, together with a square-root power-law fit (solid line) [see Eq. (2)].

IV. TRANSITION BETWEEN SPIN-LIQUID AND FERROMAGNETIC PHASES

We now turn to the discussion of the SL-F transition. The phase transition may be characterized by the behavior of the total magnetization per site m, as illustrated in Fig. 6 for $D = 0$, with the SL phase being of the $(IC)_2$ type. Obviously, the iDMRG data may well be fitted to the form

$$1 - m \propto (B_c/J - B/J)^{1/2}, \qquad (2)$$

where B_c is the critical field of the SL-F transition. Indeed, we did a χ^2 fit of the (i)DMRG data in the range between $11.7 \lesssim B/J \lesssim 12.0$ to Eq. (2), determining the proportionality factor and the critical field $B_c \approx 12.0$. Further away from the transition, pronounced deviations from the simple power law are observed (see Fig. 6). Note that, in the $(IC)_2$ region of the SL phase, one has $1 - m \propto q$. Hence, Eq. (2) corresponds to the well-known Pokrovsky-Talapov[28] square-root power law for the wave number q, describing the C-IC transition in two-dimensional classical systems with uniaxial spatial anisotropy. Indeed, it seems tempting and reasonable[23,29,30] to associate the SL-F transition for the quantum spin chain with that universality class.

V. SUMMARY

In summary, studying ground-state properties of the $S = 1$ anisotropic Heisenberg antiferromagnetic chain, using mainly the iDMRG approach, we present evidence for the spin-liquid to supersolid transition being in the two-dimensional Ising and for the SL-F transition being in the Pokrovsky-Talapov universality classes. The findings are in accordance with general considerations relating quantum phase transitions in d dimensions to those in related classical systems in $(d + 1)$ dimensions.

Analyzing longitudinal two-spin and transverse two- and four-spin-correlation functions, the spin-liquid phase has been characterized in detail. Especially, the phase is found to consist of commensurate and two distinct incommensurate regions, with different dependencies of the wave number on the magnetization. Moreover, one of the incommensurate phases can be subdivided into regions of ferroquadrupolar and spin-density-wave ordering.

ACKNOWLEDGMENTS

[1]T. Tonegawa, K. Okunishi, T. Sakai, and M. Kaburagi, Prog. Theor. Phys. Suppl. **159**, 77 (2005).

[2]P. Sengupta and C. D. Batista, Phys. Rev. Lett. **99**, 217205 (2007).

[3]D. Peters, I. P. McCulloch, and W. Selke, Phys. Rev. B **79**, 132406 (2009).

[4]D. Peters, I. P. McCulloch, and W. Selke, J. Phys: Conf. Ser. **200**, 022046 (2010).

[5]D. Rossini, V. Giovannetti, and R. Fazio, Phys. Rev. B **83**, 140411(R) (2011).

[6]M. Holtschneider and W. Selke, Phys. Rev. B **76**, 220405(R) (2007); Eur. Phys. J. B **62**, 147 (2008).

[7]P. Zhou, G. F. Tuthill, and J. E. Drumheller, Phys. Rev. B **45**, 2541 (1992).

[8]S. Kimura, T. Takeuchi, K. Okunishi, M. Hagiwara, Z. He, K. Kindo, T. Taniyama, and M. Itoh, Phys. Rev. Lett. **100**, 057202 (2008).

[9]S. Wessel and M. Troyer, Phys. Rev. Lett. **95**, 127205 (2005).

[10]K.-K. Ng and T. K. Lee, Phys. Rev. Lett. **97**, 127204 (2006).

[11]N. Laflorencie and F. Mila, Phys. Rev. Lett. **99**, 027202 (2007).

[12]A. V. Sizanov and A. V. Syromyatnikov, Phys. Rev. B **84**, 054445 (2011).

[13]L. Seabra and N. Shannon, Phys. Rev. B **83**, 134412 (2011).

[14]J. Romhanyi, F. Pollmann, and K. Penc, Phys. Rev. B **84**, 184427 (2011).

[15]Z. Nussinov, Physics **1**, 40 (2008).

[16]J. M. Kosterlitz, D. R. Nelson, and M. E. Fisher, Phys. Rev. B **13**, 412 (1976).

[17]H. Matsuda and T. Tsuneto, Prog. Theoret. Phys. Suppl. **46**, 411 (1970).

[18]K.-S. Liu and M. E. Fisher, J. Low. Temp. Phys. **10**, 655 (1973).

[19]T. Matsubara and H. Matsuda, Prog. Theor. Phys. **16**, 569 (1956).

[20]S. R. White, Phys. Rev. B **48**, 10345 (1993).

[21]U. Schollwöck, Rev. Mod. Phys. **77**, 259 (2005).

[22]I. P. McCulloch, J. Stat. Mech.: Theory and Experiment (2007) P10014; e-print arXiv:0804.2509 (2008).

[23]M. Suzuki, Prog. Theoret. Phys. **56**, 1454 (1976).

[24]T. Giamarchi and A. M. Tsvelik, Phys. Rev. B **59**, 11398 (1999).

[25]A. Läuchli, F. Mila, and K. Penc, Phys. Rev. Lett. **97**, 087205 (2006).

[26]S. R. Manmana, A. M. Läuchli, F. H. L. Essler, and F. Mila, Phys. Rev. B **83**, 184433 (2011).

[27]D. Peters, Ph.D. thesis, RWTH Aachen University, 2011.

[28]V. L. Pokrovsky and A. L. Talapov, Phys. Rev. Lett. **42**, 65 (1979).

[29]D. C. Cabra, A. Honecker, and P. Pujol, Phys. Rev. B **58**, 6241 (1998).

[30]H. J. Schulz, Phys. Rev. B **34**, 6372 (1986).